



NRC Publications Archive Archives des publications du CNRC

Photoluminescence and Raman scattering in axial Si/Ge nanowire heterojunctions

Chang, H.-Y.; Tsybeskov, L.; Sharma, S.; Kamins, T.I.; Wu, X.; Lockwood, D. J.

This publication could be one of several versions: author's original, accepted manuscript or the publisher's version. / La version de cette publication peut être l'une des suivantes : la version prépublication de l'auteur, la version acceptée du manuscrit ou la version de l'éditeur.

For the publisher's version, please access the DOI link below. / Pour consulter la version de l'éditeur, utilisez le lien DOI ci-dessous.

Publisher's version / Version de l'éditeur:

<https://doi.org/10.1063/1.3240595>

Applied physics letters, 95, 13, 2009

NRC Publications Record / Notice d'Archives des publications de CNRC:

<https://nrc-publications.canada.ca/eng/view/object/?id=ee4a74cd-330a-4477-aad2-204d173cc9a3>

<https://publications-cnrc.canada.ca/fra/voir/objet/?id=ee4a74cd-330a-4477-aad2-204d173cc9a3>

Access and use of this website and the material on it are subject to the Terms and Conditions set forth at

<https://nrc-publications.canada.ca/eng/copyright>

READ THESE TERMS AND CONDITIONS CAREFULLY BEFORE USING THIS WEBSITE.

L'accès à ce site Web et l'utilisation de son contenu sont assujettis aux conditions présentées dans le site

<https://publications-cnrc.canada.ca/fra/droits>

LISEZ CES CONDITIONS ATTENTIVEMENT AVANT D'UTILISER CE SITE WEB.

Questions? Contact the NRC Publications Archive team at

PublicationsArchive-ArchivesPublications@nrc-cnrc.gc.ca. If you wish to email the authors directly, please see the first page of the publication for their contact information.

Vous avez des questions? Nous pouvons vous aider. Pour communiquer directement avec un auteur, consultez la première page de la revue dans laquelle son article a été publié afin de trouver ses coordonnées. Si vous n'arrivez pas à les repérer, communiquez avec nous à PublicationsArchive-ArchivesPublications@nrc-cnrc.gc.ca.



Photoluminescence and Raman scattering in axial Si/Ge nanowire heterojunctions

H.-Y. Chang,¹ L. Tsybeskov,^{1,a)} S. Sharma,² T. I. Kamins,² X. Wu,³ and D. J. Lockwood³

¹Department of ECE, New Jersey Institute of Technology, Newark, New Jersey 07102-1982, USA

²Information and Quantum Systems Laboratory, Hewlett-Packard Laboratories, Palo Alto, California 94304, USA

³Institute for Microstructural Sciences, National Research Council, Ottawa, Ontario K1A 0R6, Canada

(Received 2 June 2009; accepted 10 September 2009; published online 1 October 2009)

In crystalline, dislocation-free, Si/Ge nanowire axial heterojunctions grown using the vapor-liquid-solid technique, photoluminescence and Raman spectroscopy reveal a SiGe alloy transition layer with preferential chemical composition and strain. In addition to the lattice mismatch, strain in Si/Ge nanowires is observed from a temperature dependent study to be affected by the difference in Si and Ge thermal expansion. The conclusions are supported by analytical transmission electron microscopy measurements. © 2009 American Institute of Physics.

[doi:10.1063/1.3240595]

It is well known that conventional Ge heteroepitaxy on Si is complicated by the 4.2% difference in Ge and Si lattice constants.^{1,2} Proven techniques for building quality Si/Ge heterojunctions (HJs) include multistep annealing to relax the Ge layer,³ two-dimensional (2D) growth (i.e., thin films) using Si_{1-x}Ge_x alloy transition layers with graded Ge composition x ,^{1,2,4} and three-dimensional (3D) growth in the form of SiGe clusters using the Stranski–Krastanov growth mode.^{1,2,5} Another interesting possibility is to use one-dimensional growth in the form of nanowires (NWs) produced by vapor-liquid-solid (VLS) growth or similar techniques.^{6–9} Compared to 2D and 3D nanostructures, NWs may have Si/Ge HJs with different geometries, for example, axial Si/Ge NW HJs, where the Si/Ge heterointerfaces are perpendicular to the NW axes and radial “core-shell” NW HJs, where the Si/Ge heterointerfaces are parallel to the NW axes.^{9–11} In axial Si/Ge NW HJs, strain created by the lattice mismatch between Si and Ge can partially be relieved at the heterointerfaces by the lateral displacement of atoms in small-diameter NWs.^{12,13} Thus, the fabrication and study of Si/Ge NW HJ properties could open interesting opportunities in building defect-free nanodevices.

In addition to high-resolution transmission electron microscopy (TEM),¹² photoluminescence (PL) and Raman scattering measurements can provide critical information about the Si/SiGe HJ structural properties, including the presence of dislocations by detecting specific PL lines (e.g., D-lines, etc.),^{14–16} the chemical composition, and the strain at the heterointerfaces.^{5,17} In this work we present results of Raman and PL studies convincingly demonstrating strong spontaneous intermixing in axial Si/Ge NW HJs with preferential SiGe compositions and strain, which is due to the VLS NW formation process, as well as to the differences in Si and Ge lattice constants and their thermal expansion.

The Si/Ge NW HJ samples for this work were grown using the VLS technique, Au catalysts, and the thermal decomposition of silane (SiH₄) and germane (GeH₄). The NW HJs were grown in a reduced-pressure, lamp-heated, chemical vapor deposition (CVD) reactor. The substrate was p -type

Si(111) with a resistivity of 0.01–0.02 Ω cm. A thin layer of Au was deposited on the cleaned Si substrate and annealed in the CVD reactor for 10 min at 670 °C at 95 Torr in a H₂ ambient. The Si segments of the NWs were grown at 680 °C at 30 Torr using the gaseous precursors SiH₄ and HCl in a H₂ ambient. The sample was cooled to 350 °C at a nominal rate of 75 °C/min with the SiH₄–HCl–H₂ mixture flowing. The Ge segments of the NWs were then grown at 350 °C and 90 Torr, using GeH₄ and HCl as the gaseous precursors in the H₂ ambient.

Raman scattering was performed using a double grating, 1 m focal length Raman spectrometer. In the PL measurements, the sample was held in a closed-cycle cryostat operating at temperatures in the range of 10–300 K. The PL signal was dispersed using a single-grating Acton Research 0.5 m focal length monochromator and detected by a thermoelectrically cooled InGaAs photomultiplier. Analytical TEM measurements were performed in a JEOL JEM-2100F field emission source TEM operated at 200 kV with the chemical composition studied quantitatively by energy-dispersive x-ray spectroscopy (EDX) using an Oxford INCA Energy TEM 200 with a probe size of 0.7 nm.

A TEM micrograph of a Si/Ge NW HJ is shown in the inset of Fig. 1. The clearly visible NW diameter expansion near the transition from Si to Ge are, most likely, related to the effect of the 4.2% lattice constant mismatch and the different thermal contractions of Si and Ge between their growth temperatures and room temperature. Raman scattering measurements (Fig. 1) confirm the presence of Ge in the NWs (Raman peak at 300 cm⁻¹) as well as strong SiGe intermixing (a peak near 400 cm⁻¹). Also, a broad Raman peak near 500 cm⁻¹ associated with Si–Si vibration in SiGe indicates a nonuniform strain,¹⁸ while the Raman signal associated with the Si substrate is found at 520 cm⁻¹ (Fig. 1).

Figure 2 compares the normalized Si/Ge NW PL spectra to the c -Si PL spectrum measured at the same ($T=20$ K) temperature. The Si/Ge NW PL spectra clearly exhibit at least two peaks (a narrower PL peak at ~ 1.08 eV, and a broader PL peak at ~ 1.025 eV) and, no significant PL with photon energies close to the bulk c -Si transverse optical (TO) PL peak at ~ 1.1 eV. The relative intensities of the two

^{a)}Electronic mail: tsybesko@adm.njit.edu.

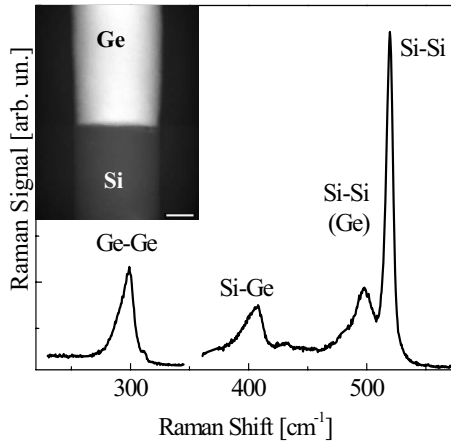


FIG. 1. Raman spectrum of Si/Ge NW HJs collected under 458 nm excitation of an Ar⁺ laser. The inset shows a TEM micrograph of a wire sample with a 20 nm length-scale bar.

Si/Ge NW PL peaks are found to be excitation and temperature dependent (Figs. 2 and 3). Measuring the Si/Ge NW PL temperature dependence, we find that the broader PL peak at ~ 1.025 eV is actually comprised of two peaks, which is most clearly seen at $T \geq 60$ K, with the peak positions at ~ 0.96 and ~ 1.0 eV (Fig. 3). The ~ 1.08 eV PL peak exhibits an asymmetric broadening at higher temperatures ($T \geq 60$ K), which can be well fitted using Boltzmann thermal broadening on the high photon energy side of the PL spectrum.¹⁹ The PL peaks at ~ 1.08 eV and 0.96 eV do not change their positions significantly with temperature, while the PL peak at ~ 1.0 eV shifts nonmonotonically and exhibits the lowest photon energy between 60 and 80 K.

The absence of bulk, *c*-Si TO phonon PL at 1.1 eV indicates that in a heavily doped Si substrate the PL is suppressed by Auger processes. The PL related to pure *c*-Ge is outside of the detector sensitivity spectral range. Thus, the observed PL (Figs. 2 and 3) is associated with radiative transitions in Si/Ge NW HJs. Since no PL associated with D-lines is observed, we conclude that these Si/Ge nanostructures are substantially dislocation-free, as confirmed from TEM analysis. The PL peak at ~ 1.08 eV is ~ 20 meV redshifted and strongly broadened when compared to the *c*-Si PL spectrum (Fig. 2), indicating, in agreement with the Raman data and theoretical analysis in Ref. 13, significant strain in the Si/Ge NWs. The PL at $h\nu \leq 1.0$ eV indicates

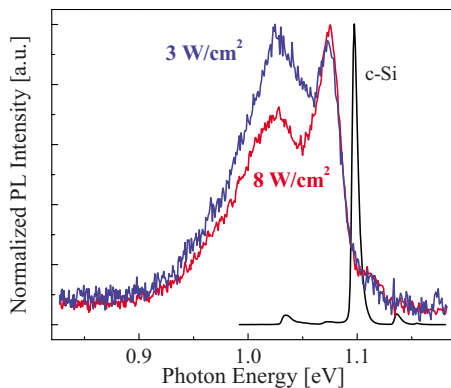


FIG. 2. (Color online) Low temperature ($T=20$ K) normalized PL spectra of Si/Ge NW HJs recorded under two different excitation intensities, as indicated. The normalized PL spectrum of *c*-Si is shown for comparison.

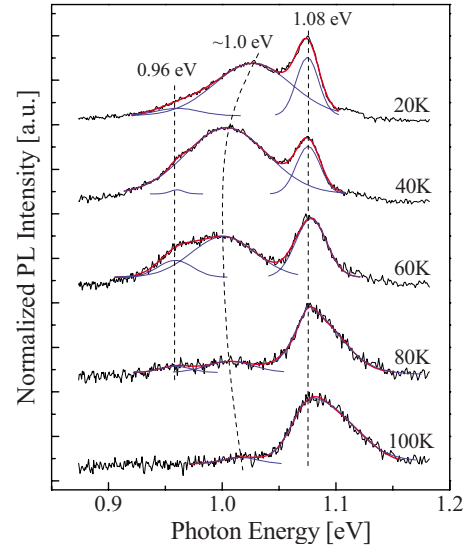


FIG. 3. (Color online) Normalized PL spectra of Si/Ge NW HJs measured under 8 W/cm^2 excitation intensity at different (indicated) temperatures with the fitted PL peaks and marked peak positions. The PL spectra are shifted vertically for clarity.

spontaneous formation of $\text{Si}_{1-x}\text{Ge}_x$ alloys between the Si and Ge parts of the NWs. Based on the strain introduced into the Si NW part, which can be estimated from the strained Si PL peak spectral position (the PL peak at ~ 1.08 eV), we find $x \leq 20\%$. Indeed, the PL peak at ~ 1.0 eV corresponds to bandgap PL in a strained $\text{Si}_{1-x}\text{Ge}_x$ alloy on (111) Si with an alloy composition close to $x \approx 15\% - 20\%$.^{1,2,20} Since the PL peaks at ~ 0.96 and ~ 1.0 eV show different temperature dependences, they are not associated with TO-phonon replica and no-phonon PL, which is frequently observed in SiGe alloys.^{1,2} Most likely, the PL peaked at ~ 0.96 eV corresponds to the bandgap of a $\text{Si}_{1-x}\text{Ge}_x$ alloy with $x \approx 0.5$.^{1,2}

The spontaneous SiGe intermixing found in VLS grown Si/Ge NW HJs is, most likely, due to residual Si atoms in the eutectic Si–Au alloy after switching to Ge deposition and to strain-induced Si and Ge interdiffusion caused by the 4.2% lattice mismatch between Si and Ge. Our PL data show that the concentration gradient from Si to Ge within the VLS grown Si/Ge NW HJ is not constant and that the $\text{Si}_{1-x}\text{Ge}_x$ alloy composition x does not change uniformly from 0 to 1. Instead, the PL data suggests the formation of $\text{Si}_{1-x}\text{Ge}_x$ alloys with preferential compositions of $x \sim 0.15 - 0.2$ close to the Si part of the Si/Ge NW and $x \approx 0.5$ close to the Ge part of the Si/Ge NW. This conclusion, supported by our preliminary TEM and EDX analysis (Figs. 1 and 4, insets), is also in agreement with the PL data and SiGe composition measurements in Si/ $\text{Si}_{1-x}\text{Ge}_x$ 3D (i.e., cluster morphology) nanostructures where $x \approx 0.2$ is a typical composition of the SiGe wetting layer and $x \leq 0.5$ is a stable composition close to the SiGe cluster core.^{2,5,14,20}

Figure 4 supports this conclusion by showing that the PL peak at ~ 1.0 eV exhibits an unusual non-monotonic temperature-dependence with a minimum at around 60–80 K. We suggest that this shift is produced by a change in Si/Ge NW strain due to the large difference in Si and Ge coefficients of thermal expansion (CsTE). Specifically, as the temperature increases from 20 to 120 K, the Si CTE first decreases and then increases, with a minimum around 60–80 K, while the Ge CTE monotonically increases.²¹ The PL

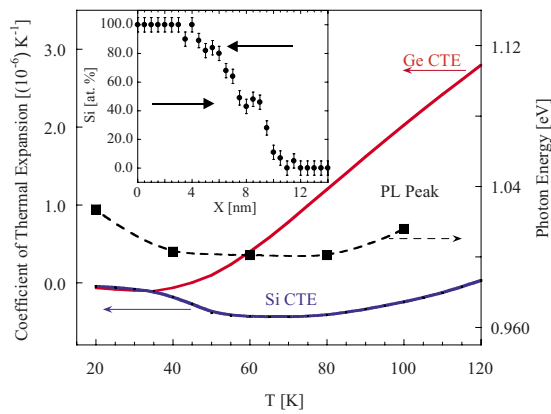


FIG. 4. (Color online) Temperature dependence of the PL peak near 1.0 eV in comparison with the temperature dependences of Si and Ge coefficients of thermal expansion. The inset shows representative EDX data along the NW axis with arrows pointing to the expected preferential compositions of ~ 80 and 50 at. % of Si within the SiGe NW HJs.

peak at ~ 1.0 eV, which we relate to a strained $\text{Si}_{1-x}\text{Ge}_x$ alloy ($x \approx 0.15-0.2$) near the Si part of the Si/Ge NW, follows the direction of the *c*-Si CTE temperature dependence (Fig. 4), while the PL peak (at ~ 0.96 eV) associated with $\text{Si}_{1-x}\text{Ge}_x$ alloy near the Ge part of the NW ($x \approx 0.5$) does not show this behavior. Thus, the mismatch in Si and Ge CsTE creates an additional, temperature-dependent strain in the Si/Ge NW HJs.

In conclusion, we show that axial Si/Ge NW HJs can be grown dislocation-free without traditional limitations in lattice-mismatched heterostructure critical thicknesses. The Raman, PL, and EDX measurements show the spontaneous formation of $\text{Si}_{1-x}\text{Ge}_x$ alloys between the Si and Ge parts of the NW HJs and indicate preferential alloy compositions of $x \approx 0.15-0.2$ (close to the Si NW part) and $x \approx 0.5$ (close to the Ge NW part). The mismatch in Si and Ge CsTE is found to be responsible for additional strain and an unusual PL peak shift as a function of temperature.

The work at NJIT is supported in part by National Science Foundation ECCS-0725443, U. S. Army Research Office W911F-09-1-01-89, and Foundation at NJIT. The samples were grown at Hewlett-Packard Laboratories. We thank G. Parent for TEM sample preparation and J.W. Fraser for scanning electron microscopy measurements.

- ¹D. J. Paul, *Semicond. Sci. Technol.* **19**, R75 (2004).
- ²K. Brunner, *Rep. Prog. Phys.* **65**, 27 (2002).
- ³A. K. Okyay, A. M. Nayfeh, K. C. Saraswat, T. Yonehara, A. Marshall, and P. C. McIntyre, *Opt. Lett.* **31**, 2565 (2006).
- ⁴F. K. LeGoues, B. S. Meyerson, and J. F. Morar, *Phys. Rev. Lett.* **66**, 2903 (1991).
- ⁵B. V. Kamenev, H. Grebel, L. Tsybeskov, T. I. Kamins, R. S. Williams, J. M. Baribeau, and D. J. Lockwood, *Appl. Phys. Lett.* **83**, 5035 (2003).
- ⁶R. S. Wagner, in *Whisker Technology*, edited by A. P. Levitt (Wiley, New York, 1970), pp. 47-119.
- ⁷T. I. Kamins, X. Li, R. S. Williams, and X. Liu, *Nano Lett.* **4**, 503 (2004).
- ⁸J. B. Hannon, S. Kodambaka, F. M. Ross, and R. M. Tromp, *Nature (London)* **440**, 69 (2006).
- ⁹N. D. Zakharov, P. Werner, G. Gerth, L. Schubert, L. Sokolov, and U. Gösele, *J. Cryst. Growth* **290**, 6 (2006).
- ¹⁰L. J. Lauhon, M. S. Gudiksen, D. Wang, and C. M. Lieber, *Nature (London)* **420**, 57 (2002).
- ¹¹J. Xiang, W. Lu, Y. Hu, Y. Wu, H. Yan, and C. M. Lieber, *Nature (London)* **441**, 489 (2006).
- ¹²Y. Li, F. Qian, J. Xiang, and C. M. Lieber, *Mater. Today* **9**, 18 (2006).
- ¹³E. Ertekin, P. A. Greaney, D. C. Chrzan, and T. D. Sands, *J. Appl. Phys.* **97**, 114325 (2005).
- ¹⁴D. J. Lockwood, J. M. Baribeau, B. V. Kamenev, E. K. Lee, and L. Tsybeskov, *Semicond. Sci. Technol.* **23**, 064003 (2008).
- ¹⁵R. Sauer, J. Weber, J. Stolz, E. R. Weber, K. H. Küsters, and H. Alexander, *Appl. Phys. A: Mater. Sci. Process.* **36**, 1 (1985).
- ¹⁶V. Higgs, F. Chin, X. Wang, J. Mosalski and R. Beanland, *J. Phys.: Condens. Matter* **12**, 10105 (2000).
- ¹⁷L. K. Orlov, Z. J. Horvath, N. L. Ivina, V. I. Vdovin, E. A. Steinman, M. L. Orlov, and Y. A. Romanov *Opto-Electron. Rev.* **11**, 169 (2003).
- ¹⁸S. Nakashima, T. Mitani, M. Ninomiya, and K. Matsumoto, *J. Appl. Phys.* **99**, 053512 (2006).
- ¹⁹L. Tsybeskov, K. L. Moore, D. G. Hall, and P. M. Fauchet, *Phys. Rev. B* **54**, R8361 (1996).
- ²⁰B. V. Kamenev, L. Tsybeskov, J. M. Baribeau, and D. J. Lockwood, *Appl. Phys. Lett.* **84**, 1293 (2004).
- ²¹R. R. Reeber and K. Wang, *Mater. Chem. Phys.* **46**, 259 (1996).